

REPORT DOCUMENTATION PAGE					Form Approved OMB No. 0704-0188	
<p>The public reporting burden for this collection of information is estimated to average 1 hour per response, including the time for reviewing instructions, searching existing data sources, gathering and maintaining the data needed, and completing and reviewing the collection of information. Send comments regarding this burden estimate or any other aspect of this collection of information, including suggestions for reducing the burden, to the Department of Defense, Executive Services and Communications Directorate (0704-0188). Respondents should be aware that notwithstanding any other provision of law, no person shall be subject to any penalty for failing to comply with a collection of information if it does not display a currently valid OMB control number.</p> <p>PLEASE DO NOT RETURN YOUR FORM TO THE ABOVE ORGANIZATION.</p>						
1. REPORT DATE (DD-MM-YYYY)		2. REPORT TYPE			3. DATES COVERED (From - To)	
4. TITLE AND SUBTITLE				5a. CONTRACT NUMBER		
				5b. GRANT NUMBER		
				5c. PROGRAM ELEMENT NUMBER		
6. AUTHOR(S)				5d. PROJECT NUMBER		
				5e. TASK NUMBER		
				5f. WORK UNIT NUMBER		
7. PERFORMING ORGANIZATION NAME(S) AND ADDRESS(ES)					8. PERFORMING ORGANIZATION REPORT NUMBER	
9. SPONSORING/MONITORING AGENCY NAME(S) AND ADDRESS(ES)					10. SPONSOR/MONITOR'S ACRONYM(S)	
					11. SPONSOR/MONITOR'S REPORT NUMBER(S)	
12. DISTRIBUTION/AVAILABILITY STATEMENT						
13. SUPPLEMENTARY NOTES						
14. ABSTRACT						
15. SUBJECT TERMS						
16. SECURITY CLASSIFICATION OF:			17. LIMITATION OF ABSTRACT	18. NUMBER OF PAGES	19a. NAME OF RESPONSIBLE PERSON	
a. REPORT	b. ABSTRACT	c. THIS PAGE			19b. TELEPHONE NUMBER (Include area code)	

Iron cycling at corroding carbon steel surfaces

Jason S. Lee^{a*}, Joyce M. McBeth^{b1}, Richard I. Ray^a, Brenda J. Little^a and David Emerson^b

^aNaval Research Laboratory, Stennis Space Center, MS, USA; ^bBigelow Laboratory for Ocean Sciences, East Boothbay, ME, USA

(Received 10 June 2013; accepted 15 August 2013)

Surfaces of carbon steel (CS) exposed to mixed cultures of iron-oxidizing bacteria (FeOB) and dissimilatory iron-reducing bacteria (FeRB) in seawater media under aerobic conditions were rougher than surfaces of CS exposed to pure cultures of either type of microorganism. The roughened surface, demonstrated by profilometry, is an indication of loss of metal from the surface. In the presence of CS, aerobically grown FeOB produced tight, twisted helical stalks encrusted with iron oxides. When CS was exposed anaerobically in the presence of FeRB, some surface oxides were removed. However, when the same FeOB and FeRB were grown together in an aerobic medium, FeOB stalks were less encrusted with iron oxides and appeared less tightly coiled. These observations suggest that iron oxides on the stalks were reduced and solubilized by the FeRB. Roughened surfaces of CS and denuded stalks were replicated with three culture combinations of different species of FeOB and FeRB under three experimental conditions. Measurements of electrochemical polarization resistance established different rates of corrosion of CS in aerobic and anaerobic media, but could not differentiate rate differences between sterile controls and inoculated exposures for a given bulk concentration of dissolved oxygen. Similarly, total iron in the electrolyte could not be used to differentiate treatments. The experiments demonstrate the potential for iron cycling (oxidation and reduction) on corroding CS in aerobic seawater media.

Keywords: seawater; iron-oxidizing bacteria; iron-reducing bacteria; carbon steel; microbiologically influenced corrosion

Introduction

Iron oxidizing bacteria (FeOB) were among the first groups of microorganisms identified as causing microbiologically influenced corrosion (MIC) (Sharpley 1961; Kobrin 1976). FeOB oxidize ferrous (Fe^{2+}) to ferric (Fe^{3+}) to obtain energy. The FeOB genera that are usually cited as causing MIC are neutrophilic, microaerophilic stalk- and sheath-producing, eg *Gallionella*, *Sphaerotilus*, *Crenothrix*, *Siderocapsa*, *Clonothrix*, and *Leptothrix* (Little & Lee 2007). These organisms can produce dense deposits made up of intact and/or the partly degraded remains of bacterial cells mixed with amorphous hydrous ferric oxides/hydroxides. Deposits, including those produced by FeOB, initiate a series of events that are individually or collectively very corrosive for materials that are prone to under-deposit corrosion; eg 300 series stainless steels exposed in stagnant, oxygenated, and chloride-containing waters. The area under each deposit becomes a relatively small anode compared to the large surrounding oxygenated cathode. Details of this classic MIC mechanism have been described elsewhere (Little & Lee 2007). Stalk-producing, neutrophilic *Siderocapsa* sp. (Hicks 2007; Ray et al. 2009) and *Mariprofundus* sp. ('Zetaproteobacteria') (McBeth et al. 2011) have been identified in association with localized

corrosion of carbon steel (CS) in a freshwater lake and a nearshore marine environment, respectively.

The relationship of iron-reducing bacteria (FeRB) to corrosion is not straightforward; FeRB may enhance corrosion under some circumstances or have a passivating effect on corrosion in others (Larsen et al. 1998; Dubiel et al. 2002). FeRB derive energy from reduction of Fe^{3+} in one of two ways: using an electron transport chain in anaerobic respiration, or by using Fe^{3+} as an electron sink during fermentation. FeRB can be either strict anaerobes (eg members of the Geobacteraceae) or facultative anaerobes that use oxygen, but can switch to using iron as a terminal electron acceptor under anaerobiosis (eg members of the genus *Shewanella*). Inhibitor and competition experiments suggest that Fe^{3+} is an efficient electron acceptor similar to nitrate in redox ability, capable of out-competing electron acceptors of lower potential, such as sulfate or carbon dioxide. Myers and Nealson (1988) working with *Shewanella* sp. and Lovley et al. (1987) working with *Geobacter* sp. demonstrated that solid manganese and iron oxides, respectively, could serve as electron acceptors in anaerobic respiration. Coleman et al. (1993) demonstrated that some sulfate-reducing bacteria (SRB) can reduce Fe^{3+} . Investigators have demonstrated that FeRB were located in the

*Corresponding author. Email: jason.lee@nrlssc.navy.mil

¹Current Address: Canadian Light Source Inc., 44 Innovation Blvd, Saskatoon, SK, S7N 2V3, Canada

corrosion products of iron and that microbial iron oxide reduction was an important contributor to MIC by solubilization of insoluble iron compounds and removal of iron oxides (Nealson & Little 1997).

Investigators have demonstrated a spatial relationship between FeOB and FeRB in corrosion products (Dang et al. 2011). The co-occurrence of these complementary iron-cycling bacteria in natural marine corrosion environments may influence corrosion. Experiments were designed to test the hypothesis that co-cultures of FeOB and FeRB will result in enhanced corrosion of CS in comparison with monoculture experiments or abiotic controls and that the iron oxides bound to the stalks of FeOB will be reduced by FeRB.

Methods and materials

Three independent experiments were designed (Table 1). For each experimental set, a seawater medium was used as the electrolyte. Different species of FeOB and FeRB were used in each experiment. In all cases, CS (UNS C10200) electrodes (1.59 cm dia. \times 0.16 cm thick) were exposed after having been polished to 600 grit finish.

The first experiment was conducted with the FeOB *Mariprofundus ferrooxydans* strain PV-1 (NCMA B1) and the FeRB *Geothermobacter* sp. strain HR-1 (NCMA B105) in Instant Ocean (IO, 35 g l⁻¹) (www.instantocean.com). IO (750 ml) was added to 1 l green flasks (electrochemical cells) as detailed in ASTM G5 (2004). Sodium acetate (10 mM) was added to flasks destined to contain FeRB, and vitamin and mineral solutions

were added to all flasks (Guillard & Ryther 1962; Guillard 1975). The green flasks were equipped with a Luggin probe, a saturated calomel reference electrode (SCE), a graphite counter electrode, and a CS working electrode (1 cm² exposed area) with the exposed surface vertically orientated. Electrochemical cells were autoclaved (less SCE) prior to the start of the experiment. A concentrated cell solution was prepared from 400 ml of FeOB *M. ferrooxydans* PV-1 cell culture. Ten ml of the concentrate were inoculated into each of the flasks designated for FeOB and FeOB/FeRB treatments. An aliquot (5 ml) of FeRB *Geothermobacter* sp. HR-1 cell culture was inoculated into each of the FeOB and FeOB/FeRB treatments. Polarization resistance (R_p [Ω cm²]) was measured daily over a 49 d period according to ASTM G59 (2003) using a Reference 600™ potentiostat and an ECM8™ Multiplexer (Gamry Instruments, Warminster, PA, US). Solution resistance was not accounted for during the calculation of R_p . A sterile foam stopper was placed in one port hole of each electrochemical cell allowing exchange of gas. Experiments were conducted at 25 ± 1 °C in two atmospheres: aerobic – air; anaerobic – 0.01 v/v CO₂, 10 v/v H₂, bal. N₂. The following exposures were maintained: (1) aerobic sterile control; (2) anaerobic sterile control; (3) FeOB *M. ferrooxydans* PV-1 (aerobic); (4) FeRB *Geothermobacter* sp. HR-1 (anaerobic); and (5) a combination of FeOB *M. ferrooxydans* PV-1 and FeRB *Geothermobacter* sp. HR-1 (aerobic). After two d, autoclave sterilized abiotically produced iron oxide (~0.1 g) was added to the anaerobic flask containing FeRB *Geothermobacter* sp. HR-1 to ensure the presence of iron oxides as an electron donor for the bacteria. The starting pH of the solutions was 8.5 ± 0.1 . At the conclusion of the 49 d exposure, the CS electrodes were removed and prepared for environmental scanning electron microscopy (ESEM) and energy dispersive spectroscopy (EDS) as previously described (Ray & Little 2003). After acid cleaning according to ASTM G1 (2003), CS electrodes were scanned using a Nanovea PS50 (Irvine, CA) non-contact optical profiler with a 400 μ m optical laser pen. Nanovea Professional 3D software was used to reconstruct high contrast 3D digital images of the surfaces and perform statistical analysis including volume loss, maximum/median penetration, and root mean square (RMS) roughness.

In the second set of experiments, unamended natural filtered/pasteurized (Little et al. 1987) Key West, FL, US seawater was used as the electrolyte with the FeOB *Mariprofundus* strain M34 (NCMA B20) and the FeRB *Shewanella japonica* (ATCC BAA-316). CS electrodes were autoclaved and placed in sterile 50 ml falcon tubes with 40 ml of seawater. The conically shaped bottom of the falcon tubes enabled the entire surface of the CS electrode (4.8 cm²) to be exposed to the electrolyte. The following exposures were maintained in triplicate: (1) abiotic control; (2) FeOB *Mariprofundus* sp. M34; (3)

Table 1. Experimental matrix.

Experiment	Microorganisms	Electrolyte	Temp. (°C)	Exposure period (d)
1	FeOB <i>Mariprofundus ferrooxydans</i> PV-1	IO	25 ± 1	49
	FeRB <i>Geothermobacter</i> sp. HR-1			
2	FeOB <i>Mariprofundus</i> sp. M34	Sterile Key West, FL seawater	27 ± 2	14
	FeRB <i>Shewanella japonica</i>			
3	FeOB <i>Mariprofundus</i> sp. DIS-1	ASW medium*	27 ± 1	14
	FeRB <i>Shewanella frigidimarina</i>			

*Described by Emerson and Floyd (2005).

FeRB *S. japonica*; and (4) a combination of FeOB *Mariprofundus* sp. M4 and FeRB *S. japonica*. After inoculation, tubes were capped with ambient air headspaces and incubated at $27 \pm 2^\circ\text{C}$ for 14 d. The morphology of the product corrosion was examined using ESEM. Samples were also sent to CSIRO (Floreant Park, WA, Australia) for selected area electron diffraction (SAED) and transmission electron microscopy (TEM) to determine the mineralogical characteristics.

In the third set of experiments, artificial seawater (ASW) medium described by Emerson and Floyd (2005) was used as the electrolyte with the FeOB *Mariprofundus* sp. strain DIS-1 and the FeRB *Shewanella frigidimarina* (NCIMB 400). CS electrodes were embedded in EpoThin™ epoxy resin (Buehler, Lake Bluff, IL, USA) with one face exposed (2 cm^2). Individual electrodes were placed in separate 250 ml glass bottles with the polished surface facing upwards. Bottles and associated electrodes were autoclaved simultaneously. One hundred ml of sterile (autoclaved) ASW medium were added to each bottle and the bottles were incubated for 14 d at $27 \pm 1^\circ\text{C}$. The following exposures were maintained: (1) abiotic control; (2) FeOB *Mariprofundus* sp. DIS-1; (3) FeRB *S. frigidimarina*; and (4) a combination of FeOB *Mariprofundus* sp. DIS-1 and FeRB *S. frigidimarina*. Bottles were capped with ambient air headspaces. Triplicate samples were maintained for mineralogy, light microscopy, and profilometry. The electrolyte was analyzed for aqueous Fe^{2+} , solid Fe^{2+} and Fe (total) concentrations (Stookey 1970), cell counts, pH, Eh, and heterotrophic contamination every 2–4 d with nutrient plate R2A agar checks (McBeth et al. 2011).

Results

Experiment 1

The starting pH of the solutions was 8.2 ± 0.1 after the first day of exposure, and by the end of the experiment it was 7.8 ± 0.1 . The redox potentials of the bulk water dropped rapidly in all treatments within the first day of exposure, and in the treatments incubated in the anaerobic chamber reached values $<0\text{ mV}$ (SHE corrected) within 24 h. Over the first day, bright orange corrosion products were observed on all CS surfaces exposed to aerobic conditions with and without the addition of bacteria. After 2 d, flocculant iron oxides increased in the chambers containing FeOB *M. ferrooxydans* PV-1. At the conclusion of the 49 d, the aerobic exposure with FeOB *M. ferrooxydans* PV-1 resulted in dark orange corrosion products on the CS surface, whereas corrosion products were reddish dark brown without the addition of FeOB. The corrosion products were uniform in appearance and entirely covered the CS surfaces. Twisted stalks covered with iron oxides (confirmed by EDS, data not shown) were observed on

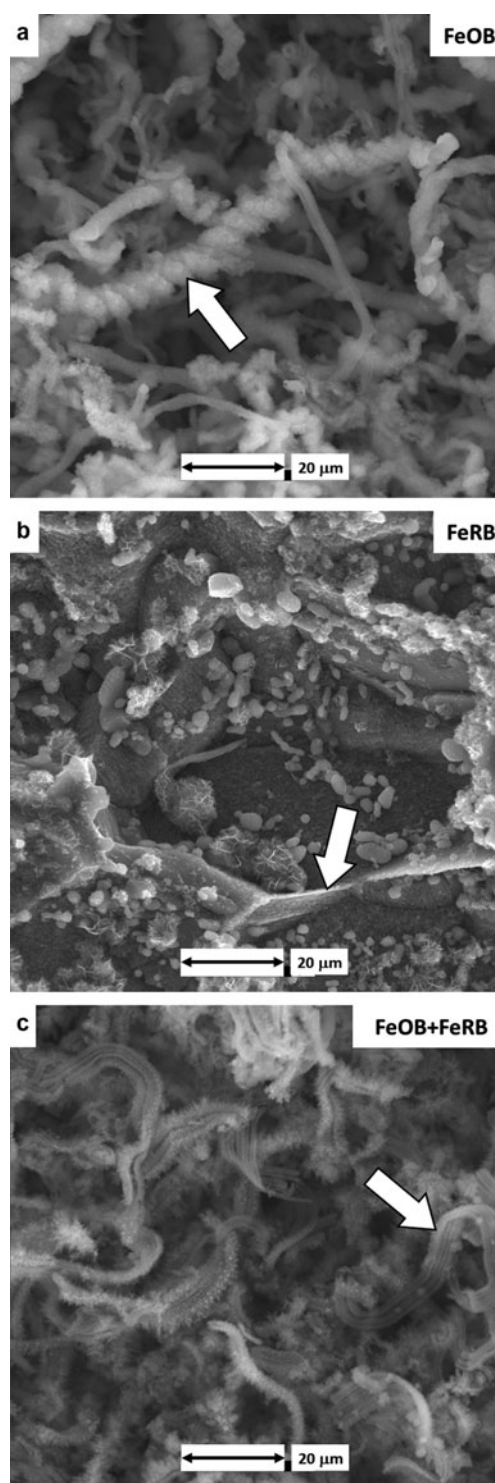


Figure 1. CS surfaces after 49 d exposures to amended IO with different bacterial additions and bulk oxygen. (a) Twisted iron oxide encrusted stalks (arrow) after aerobic exposure with FeOB *M. ferrooxydans* PV-1. (b) Remnant grain boundaries (arrow) were observed on the CS surface after anaerobic exposure with FeRB *Geothermobacter* sp. HR-1. (c) Denuded stalks (arrow) under aerobic conditions with co-cultures of FeOB *M. ferrooxydans* PV-1 and FeRB *Geothermobacter* sp. HR-1.

the CS surface after exposure to FeOB *M. ferrooxydans* PV-1 (Figure 1a). CS surfaces exposed to anaerobic conditions with and without the addition of FeRB *Geothermobacter* sp. HR-1 were dark gray throughout the 49 d exposure. Grain matrices were preferentially attacked with visible grain boundary remnants (Figure 1b). Macroscopic bright orange nodules (<1 mm diameter) covered the CS surface exposed aerobically with co-cultures of FeOB *M. ferrooxydans* PV-1 and FeRB *Geothermobacter* sp. HR-1. Stalks were observed on the nodules but were less twisted and denuded of iron oxides (Figure 1c) compared to the FeOB-only exposure (Figure 1a).

Qualitative visual comparison of surface reconstructions and line scans (Figure 2) revealed readily apparent differences among the CS surfaces exposed under different conditions. CS exposed to a combination of FeOB *M. ferrooxydans* PV-1 and FeRB *Geothermobacter* sp. HR-1 appeared rougher than CS exposed to either microorganism individually. This observation was supported by quantitative statistical analysis that showed RMS roughness was highest (12.1 μm) for CS exposed to a combination of FeOB *M. ferrooxydans* PV-1 and FeRB *Geothermobacter* sp. HR-1. In comparison, values of RMS roughness for CS exposed to individual cultures of FeOB *M. ferrooxydans* PV-1 (RMS = 10.2 μm) or FeRB *Geothermobacter* sp. HR-1 (RMS = 2.3 μm) were lower. Measurements of the RMS roughness of the pre-exposed CS surfaces with 600 grit finish were consistently low ($0.9 \pm 0.1 \mu\text{m}$). Less metal loss, as measured by profilometry, occurred in the anaerobic exposures with (0.665 mm^3) and without bacteria (0.711 mm^3). Anaerobic conditions resulted in uniform attack across the CS surfaces. The mean penetration depths across the exposed surfaces were 7.6 and 6.8 μm for anaerobic exposures with and without FeRB *Geothermobacter* sp. HR-1, respectively. The maximum penetration depths were also similar, 17.9 and 18.7 μm , for anaerobic exposures with and without FeRB *Geothermobacter* sp. HR-1, respectively. In comparison, more metal loss and deeper (max) penetration were observed in aerobic exposures with (1.94 mm^3 , 39.2 μm) and without FeOB *M. ferrooxydans* PV-1 (2.57 mm^3 , 61.7 μm), but attack was also uniform. The aerobic exposure with co-cultures of FeOB *M. ferrooxydans* PV-1 and FeRB *Geothermobacter* sp. HR-1 had a distinctive corrosion morphology where regions of deep attack (58.0 μm max) were surrounded by lightly penetrated metal (<5 μm), resulting in the roughened surface.

Table 2 shows the R_p measurements for each exposure condition averaged over the entire 49 days exposure. R_p measurements established differences between CS maintained in aerobic ($10^2 \Omega \text{ cm}^2$) and anaerobic ($10^5 \Omega \text{ cm}^2$) media, but did not differentiate (according to standard deviations) between exposures with and without addition of bacteria. Aerobic conditions produced the highest rate of corrosion (R_p^{-1}).

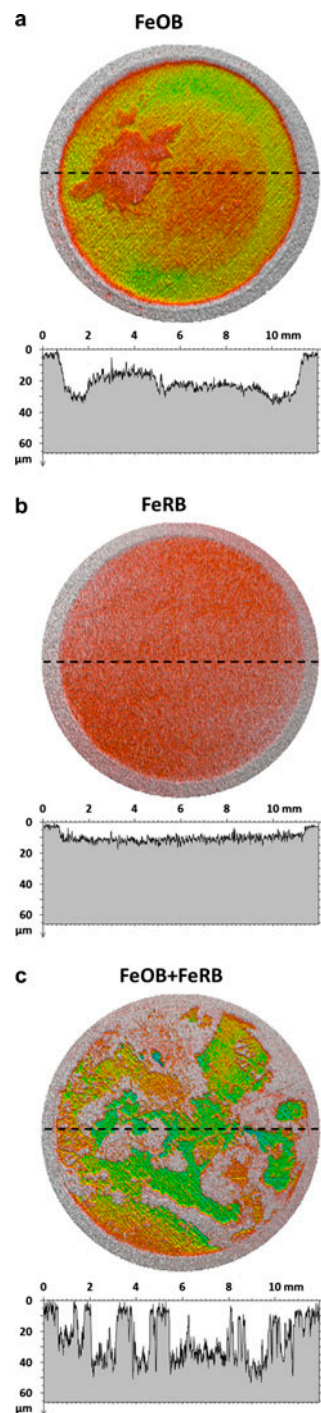


Figure 2. 3D profilometry representations of CS surfaces after 49 d exposure under different oxygen conditions and bacterial additions in amended IO. Dashed lines indicate locations of associated extracted line scan profiles. Areas with little to no attack are represented as gray. (a) Uniform morphology of corrosion after aerobic exposure with FeOB *M. ferrooxydans* PV-1. (b) Light uniform corrosion after anaerobic exposure with FeRB *Geothermobacter* sp. HR-1. (c) Roughened surface with areas of deep attack surrounded by unattacked metal after exposure to aerobic conditions with co-cultures of FeOB *M. ferrooxydans* PV-1 and FeRB *Geothermobacter* sp. HR-1.

Table 2. Average polarization resistance (R_p) of CS in IO with varying oxygen conditions and inocula over 49 d exposures.

Microorganisms	Atmosphere	Average R_p ($\Omega \text{ cm}^2$)	SD ($\Omega \text{ cm}^2$)
Sterile control	Anaerobic	1.12×10^5	0.38×10^5
FeRB	Anaerobic	1.91×10^5	0.22×10^5
<i>Geothermobacter</i> sp. HR-1			
Sterile control	Aerobic	4.05×10^2	0.79×10^2
FeOB <i>Mariprofundus</i>	Aerobic	5.15×10^2	1.27×10^2
<i>ferrooxydans</i> PV-1			
FeOB + FeRB	Aerobic	4.60×10^2	0.60×10^2

Experiment 2

CS exposed to FeOB *Mariprofundus* sp. M34 and FeRB *S. japonica* in unamended sterilized Key West seawater for 14 d produced similar results to the exposures in Experiment 1. Twisted iron oxide encrusted stalks were observed when FeOB *Mariprofundus* sp. M34 was exposed to CS (Figure 3a). Addition of FeRB *S. japonica* resulted in the presence of denuded stalks that remained tightly coiled (Figure 3b). Stalks were not observed in abiotic controls or in the exposure with FeRB *S. japonica* only.

Analysis by SEM/TEM/SAED of corrosion products on the surfaces of CS demonstrated differences between the exposure conditions. Corrosion products in the abiotic control were predominantly hematite (Figure 4a). The presence of FeOB *Mariprofundus* sp. M34 resulted in goethite with simple morphology and no long crystals or twining (Figure 4b). Exposure of CS with FeRB *S. japonica* resulted in multiple iron oxides, including goethite, lepidocrocite, magnetite, and hematite (Figure 4c). Exposure of CS with both FeOB *Mariprofundus* sp. M34 and FeRB *S. japonica* produced goethite with a number of different crystal morphologies including some long twined crystals (Figure 4d).

Experiment 3

Iron oxide encrusted stalks were observed in all exposures containing FeOB *Mariprofundus* sp. DIS-1, and abundant cells were observed in all exposures containing FeOB *Mariprofundus* sp. DIS-1 and/or FeRB *S. frigidimarina*. No cells were observed in the abiotic controls. Nutrient plate agar checks for heterotrophic contamination showed that the abiotic and FeOB *Mariprofundus* sp. DIS-1 exposures remained sterile and axenic, respectively, over the course of the experiment. FeRB *S. frigidimarina* grew on the nutrient plates; however, no colonies other than those matching FeRB *S. frigidimarina* were observed. The pH conditions in the experiments were initially 6.7 ± 0.1 and increased by the end of the

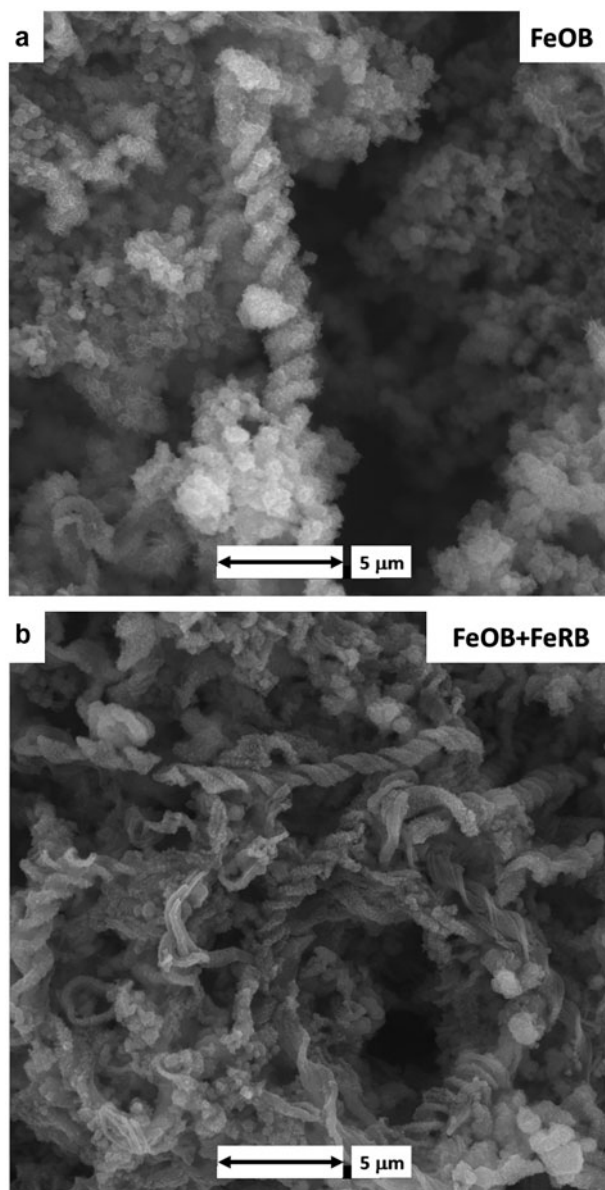


Figure 3. CS surfaces after 14 d exposures to filter sterilized Key West seawater with different bacterial additions. (a) Twisted iron oxide encrusted stalks after exposure with FeOB *Mariprofundus* sp. M34. (b) Denuded stalks after exposure with co-cultures of FeOB *Mariprofundus* sp. M34 and FeRB *S. japonica*.

experiment to 7.8 ± 0.1 (abiotic and FeOB *Mariprofundus* sp. DIS-1) and 7.2 ± 0.1 (FeRB *S. frigidimarina*, and FeOB *Mariprofundus* sp. DIS-1 + FeRB *S. frigidimarina*). The redox potentials of the bulk water (SHE corrected) ranged between +490 and +650 mV for abiotic and FeOB *Mariprofundus* sp. DIS-1 exposures over the course of the experiment; in the FeRB *S. frigidimarina* and FeOB *Mariprofundus* sp. DIS-1 + FeRB *S. frigidimarina* exposures the redox potential decreased from +500

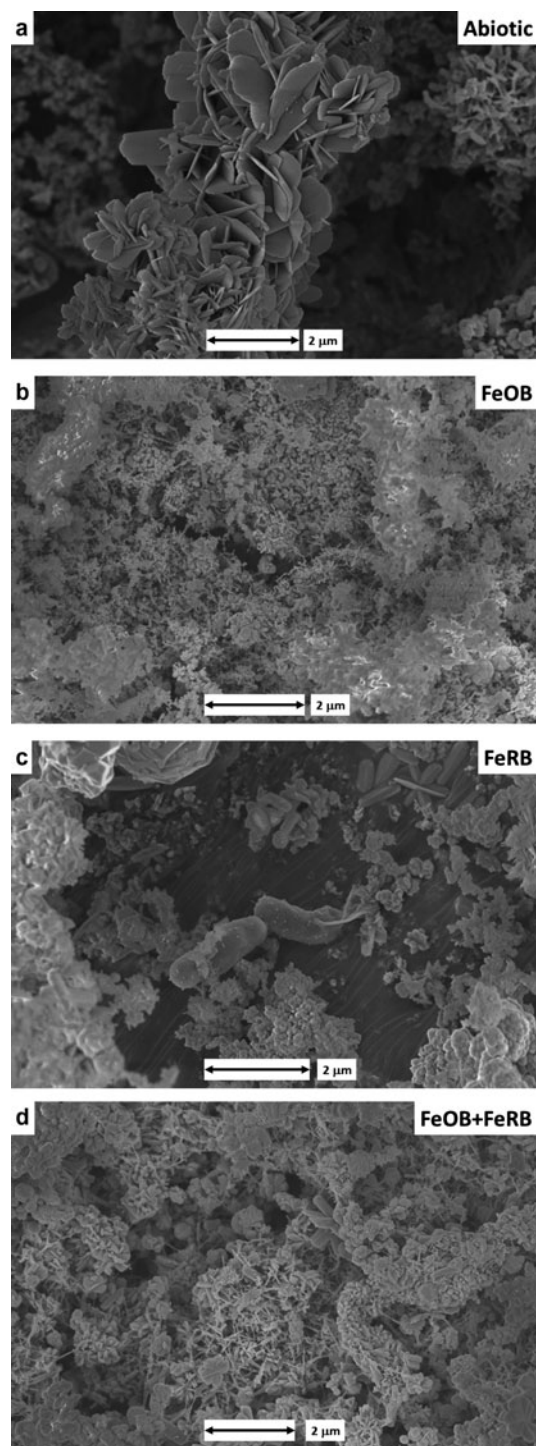


Figure 4. SEM images of the CS surfaces after 14 d exposure to filter sterilized Key West seawater with and without the addition of FeOB *Mariprofundus* sp. M34 and FeRB *S. japonica*. Mineral identification of the corrosion product section performed by TEM/SAED analysis. (a) Hematite in abiotic control; (b) goethite-only with simple morphology and no long crystal or twinning with addition of FeOB; (c) goethite, lepidocrocite, magnetite, and hematite with the addition of FeRB; and (d) goethite-only with multiple crystal morphologies, including long twinned crystals with co-cultures of FeOB and FeRB.

to +150 mV by the end of the 14 d exposure. Aqueous iron in the electrolyte was lower in the abiotic and FeOB *Mariprofundus* sp. DIS-1 exposures than in those containing FeRB *S. frigidimarina*. However, the increase in total iron (particulate and aqueous) over the 14 d period was too low to indicate trends between the types of treatment.

Coupon samples in exposures containing FeRB *S. frigidimarina* had a darker surface coating by the end of the experiment than exposures containing abiotic and FeOB *Mariprofundus* sp. DIS-1, which were orange. The iron oxides on the surface of the FeOB *Mariprofundus* sp. DIS-1 exposures were more cohesive in appearance than those of the abiotic exposures. There was no discernible macroscopic difference between the corrosion products on the coupons containing FeRB *S. frigidimarina* and FeOB *Mariprofundus* sp. DIS-1 + FeRB *S. frigidimarina*. Light microscope analyses (Figure 5) showed iron oxide encrusted stalks in samples containing FeOB *Mariprofundus* sp. DIS-1; no stalks were observed in the abiotic or FeRB *S. frigidimarina* (alone) exposures. Samples containing FeRB *S. frigidimarina* had abundant planktonic cells and a much higher cell density was observed in these exposures than in the exposures containing FeOB *Mariprofundus* sp. DIS-1 alone.

CS exposed to a combination of FeOB *Mariprofundus* sp. DIS-1 and FeRB *S. frigidimarina* in ASW medium for 14 d exhibited similar results to the 49 d experiment with different species of FeOB and FeRB but with less penetration of metal. The distinctive roughened surface of CS was observed after exposure to both FeOB *Mariprofundus* sp. DIS-1 and FeRB *S. frigidimarina* under aerobic conditions with RMS surface roughness of 4.9 ± 0.4 µm. Regions of attack were smaller in area compared to the 49 d exposures. Pit density was low (3 pits cm⁻²) with typical pit dimensions of 250 µm diameter and 20 µm depth. Other exposures, including controls, resulted in uniform corrosion with <7 µm metal penetration and RMS roughness values <2.0 µm.

Discussion

Corrosion product mineralogy can be used to interpret the role of microorganisms in MIC (McNeil & Odom 1994). In Experiment 2 described in this paper, the corrosion products in the abiotic controls were predominantly hematite. Oxide films formed on iron in air at temperatures below 200 °C are composed of magnetite and hematite (Szklaarska-Smialowska 2005). The mineralogy of products of corrosion, in the presence of FeOB and FeRB, was consistently different from those formed in abiotic controls.

The precise conditions for the growth of microaerophilic FeOB has been the topic of extensive study. Emerson and Moyer (1997) described a gel-stabilized gradient

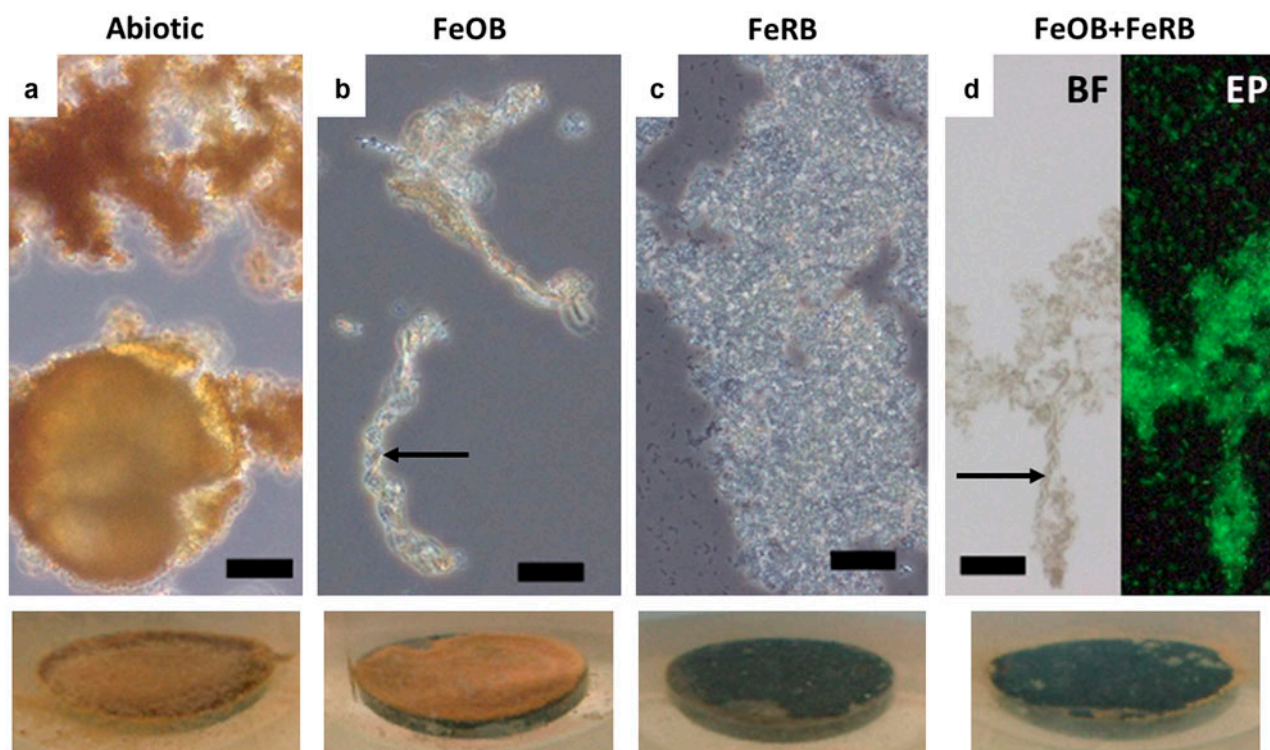


Figure 5. Light microscope images of biofilms/corrosion products after 14 d exposures in amended ASW with and without additions of FeOB *Mariprofundus* sp. DIS-1 and FeRB *S. frigidimarina*. Associated macroscopic images of surfaces of CS (1.59 cm diameter) *in situ* after 14 d are shown at the bottom. Abundant orange iron oxides were present in the abiotic controls (a), but cells were not observed in this treatment. Cells were observed in association with stalk structures of iron oxide (indicated by arrows) in treatments containing FeOB (b and d). Abiotic treatments (a) and those containing only FeRB (c) did not contain stalk structures of iron oxide. Note abundant cells of planktonic FeRB in images (c) and (d). The image (d) shows the same sample examined using brightfield (BF) and epifluorescence (EP) microscopy stained with the nucleic acid stain Syto13. Scale bars represent 10 μ m.

method that used opposing gradients of Fe^{2+} and O_2 to isolate and characterize FeOB. It is established that neutrophilic FeOB compete with rapid abiotic oxidation of Fe^{2+} and have adapted to low O_2 environments where they couple the oxidation of Fe^{2+} and reduction of O_2 . For example, Druschel et al. (2008) determined that the maximum levels of O_2 associated with the growth of *Sideroxydans lithotrophicus* were 15–50 μM . FeOB typically exist within zones of low oxygen partial pressure and high concentrations of Fe^{2+} . These conditions occur commonly at the oxic–anoxic boundary of groundwater springs (James & Ferris 2004) and in the steep redox zones surrounding macrofaunal roots in tidal marshes (Wang et al. 2011). Wang et al. (2011) reported that the distribution of FeOB in a tidal freshwater marsh did not have a simple relationship with the redox potential based on depth profiles. They indicated that oxygen-supplying macrofauna appeared to control ‘the spatial and temporal variation in FeOB communities.’

It is clear from the work presented here that FeOB can grow and proliferate on corroding CS submerged in an oxygenated medium. Corrosion reactions reduce the

level of dissolved oxygen (Lee et al. 2004), creating conditions amenable to the growth of FeOB. Support for this hypothesis is provided by McBeth et al. (2011) and Dang et al. (2011) who reported that FeOB (*Mariprofundus*) were among the first colonizers when CS was submerged in coastal seawater.

Bacteriogenic iron oxides (BIOS), formed as a result of bacterial oxidation of Fe^{2+} to Fe^{3+} , are made up of intact and/or partly degraded remains of bacterial cells mixed with amorphous hydrous Fe^{3+} oxides (Ferris 2005). Miot et al. (2009) demonstrated a redox gradient associated with FeOB *Rhodobacter* sp. strain SW2 where the highest proportion of Fe^{3+} was near the cell and the concentration of Fe^{2+} increased with distance from the cell. Several iron minerals have been identified with BIOS. The most common mineral form of BIOS is relatively amorphous two-line ferrihydrite (Langley et al. 2009; Toner et al. 2012). Banfield et al. (2000) identified 2-line ferrihydrite associated with stalks of *Gallionella* sp. and the sheath of a *Leptothrix* sp. collected from the drainage water of mines. Ferrihydrite is one of the first solid phases to form upon abiotic oxidation of ferrous

iron in neutral pH solutions. Ferrihydrite can undergo transformation to goethite and/or lepidocrocite (oxidation and hydrolysis) and hematite (internal rearrangement). Chan et al. (2011) identified lepidocrocite deposits on stalks of *Mariprofundus ferrooxydans* PV-1 grown in ASW with FeS as the source of Fe²⁺. A biopolymer was associated with the iron oxide encrusted stalks. Goethite and lepidocrocite have been identified in association with stalks of FeOB in the core regions of tubercles formed in freshwater on CS (Gerke et al. 2008; Little et al. 2010; Ray et al. 2011; Gerke et al. 2012). Miot et al. (2009) demonstrated precipitation of goethite on polymeric fibers extending from the cells of phototrophic FeOB. In the present work, goethite was identified in the corrosion products associated with the FeOB, *Mariprofundus* sp.

FeRB enhance corrosion under some circumstances and have a passivating effect under others (Little et al. 1997; Dubiel et al. 2002). Some of the reported differences can be attributed to differences in microbial species and differences in the composition of electrolyte in experiments with the same organism (Herrera & Videla 2009). In addition, there is variation in the reactivity of Fe oxides. Using synthetic Fe oxides and 10 mM ascorbic acid at pH 3, Larsen and Postma (2001) studied the kinetics of bulk reductive dissolution. They concluded that the relationship between mass and surface area of crystals, crystal size distribution, the relative density of the site, and preferential dissolution along crystalline boundaries influenced rates of dissolution. Similarly, Little et al. (1997) demonstrated that rates of reduction varied among Fe oxides exposed to the FeRB *S. putrefaciens*. Rates of dissolution, measured by atomic absorption, were slower for hematite compared to the rates of reduction for goethite and ferrihydrite under identical conditions of exposure. In the experiments described in this work, exposure of CS with FeRB *S. japonica* resulted in multiple iron oxides, including goethite, lepidocrocite, magnetite, and hematite. When both FeOB and FeRB were present, the corrosion products were predominantly goethite with several crystal morphologies.

The work described here is the first to investigate corrosion using defined mixed cultures of FeOB and FeRB. Different combinations of organisms and marine media were chosen to provide a range of experimental conditions. Two of the three FeOB, PV-1 and M-34, were isolated from Fe-rich microbial mats at Loihi Seamount and represent different strains of *M. ferrooxydans*. Strain DIS-1 was isolated directly from a steel coupon in Maine (McBeth et al. 2011) and appears to be an obligate Fe oxidizer, sharing morphological similarity to PV-1 and M-34. The two Fe reducers, *Geothermobacter* sp. HR-1 and *S. frigidimarina*, are members of the Deltaproteobacteria and Gammaproteobacteria, respectively.

Geothermobacter sp. HR-1 is obligately anaerobic whereas *S. frigidimarina* is facultative. The Fe-reducing HR-1 strain was also isolated from Loihi (Emerson 2009). Overall, diverse combinations of FeOB and FeRB did not produce substantially different corrosion, nor did natural seawater vs artificial seawater significantly alter the results of corrosion. In all three experiments, FeOB and FeRB were successfully co-cultured in an aerobic medium with corroding CS. Co-cultures caused significantly more roughening of the surface of CS compared to either FeOB or FeRB alone, or to abiotic controls.

The presence of FeOB-generated stalks and BIOS in biofilms provide a reactive mineral structure that can support the growth of FeRB and to which other bacteria adhere. BIOS are more readily reduced by other bacteria (eg FeRB and SRB) in comparison with synthetic oxides of iron (Blothe & Roden 2009; Emerson 2009; Langley et al. 2009), which may lead to enhanced growth of anaerobic colonizers. In this work, regardless of the specific FeOB used, exposure to CS resulted in iron encrusted stalks. Reduction of iron oxides bound to the stalks was visually observed in the presence of FeRB, regardless of experimental conditions. These data further demonstrate that FeOB generated BIOS can be used as electron acceptors and provide suitable conditions for the proliferation of FeRB.

Microbiological iron cycling mediated by associated populations of FeOB and FeRB that carry out oxidative and reductive pathways, respectively, is a recognized phenomenon, and has been studied most extensively in freshwater habitats (Emerson & Revsbech 1994; Straub et al. 2001; Weiss et al. 2004; Blothe & Roden 2009; Roden et al. 2012). Blothe and Roden (2009) suggested that in high iron environments, 'Such recycling is likely to take place in virtually all redox interfacial environments.' Examples of Fe cycling in the marine environment are less known. Iron cycling has been observed in a shallow hydrothermal vent system (Handley et al. 2010), and at a deep-sea vent where it appeared to be a very slow process (Emerson 2009). The work presented here indicates that axenic cultures of marine FeOB and FeRB can co-exist and have the potential to carry out iron cycling over very small spatial scales. The sharp decrease in the bulk redox potential observed in the experiments described in this paper suggests that FeRB and FeOB/FeRB consortia in association with corrosion of CS can drive the redox potential farther down than the processes of abiotic corrosion alone. Biofilms of FeOB and FeOB/FeRB forming at corrosion surfaces may provide anaerobic niches for processes of microbial reduction, such as dissimilatory reduction of Fe and reduction of sulfate, even in environments where the bulk conditions are oxic (Experiment 1). These observations may be important in the formation and mineralogy of corrosion products. Notably, when FeOB and FeRB

were present, the mineralogy of the oxides of Fe associated with the corrosion products was different.

Conclusions

Corroding CS in a marine environment provided the reduced dissolved oxygen conditions required for the growth of neutrophilic, microaerophilic FeOB and dissimilatory FeRB. The minerals formed in the presence of FeOB and FeRB on corroding CS were not predictable. The data provided visual evidence that FeRB can use the BIOS produced by FeOB as electron acceptors. The mineralogy of the oxides and oxyhydroxides produced by FeOB may determine the rate of reduction of iron by FeRB. Exposure of CS in the presence of co-cultures of FeOB and FeRB caused a measurable loss of metal from the surface of CS and greater roughening of the surface in comparison with incubations of CS with monocultures of FeOB or FeRB.

Acknowledgments

This work was supported by the Office of Naval Research (Dr L. Chrisey). NRL Publication number NRL/JA/7330-13-1801. The authors thank the TEM and SAED work by Kayley Usher (CSIRO Land and Water, WA, Australia) and Martin Saunders (CMCA), Justin Biffinger, and Lisa Fitzgerald for providing cultures of *S. japonica* and *S. frigidimarina*, as well as Irini Adaktylou for her help in isolating the *Mariprofundus* DIS-1 strain.

References

- ASTM Standard G1-03. 2003. Standard practice for preparing, cleaning, and evaluating corrosion test specimens. In: ASTM handbook 3.02 corrosion of metals; wear and erosion. West Conshohocken, PA: ASTM International; p. 17–25.
- ASTM Standard G5-94. 2004. Standard reference test method for making potentiostatic and potentiodynamic anodic polarization measurement. In: ASTM handbook 3.02 corrosion of metals; wear and erosion. West Conshohocken, PA: ASTM International; p. 45–56.
- ASTM Standard G59-97. 2003. Standard test method for conducting potentiodynamic polarization resistance measurements. In: ASTM handbook 3.02 corrosion of metals; wear and erosion. West Conshohocken, PA: ASTM International; p. 230–233.
- Banfield JF, Welch SA, Zhang HZ, Ebert TT, Penn RL. 2000. Aggregation-based crystal growth and microstructure development in natural iron oxyhydroxide biomineralization products. *Science*. 289:751–754.
- Blothe M, Roden EE. 2009. Microbial iron redox cycling in a circumneutral-pH groundwater seep. *Appl Environ Microbiol*. 75:468–473.
- Chan CS, Fakra SC, Emerson D, Fleming EJ, Edwards KJ. 2011. Lithotrophic iron-oxidizing bacteria produce organic stalks to control mineral growth: implications for biosignature formation. *ISME J*. 5:717–727.
- Coleman ML, Hedrick DB, Lovley DR, White DC, Pye K. 1993. Reduction of Fe(III) in sediments by sulfate-reducing bacteria. *Nature*. 361:436–438.
- Dang HY, Chen RP, Wang L, Shao SD, Dai LQ, Ye Y, Guo LZ, Huang GQ, Klotz MG. 2011. Molecular characterization of putative biocorroding microbiota with a novel niche detection of Epsilon- and Zeta-proteobacteria in Pacific Ocean coastal seawaters. *Environ Microbiol*. 13:3059–3074.
- Druschel GK, Emerson D, Sutka R, Suchecki P, Luther GW. 2008. Low-oxygen and chemical kinetic constraints on the geochemical niche of neutrophilic iron(II) oxidizing microorganisms. *Geochim Cosmochim Acta*. 72:3358–3370.
- Dubiel M, Hsu CH, Chien CC, Mansfeld F, Newman DK. 2002. Microbial iron respiration can protect steel from corrosion. *Appl Environ Microbiol*. 68:1440–1445.
- Emerson D. 2009. Potential for iron-reduction and iron-cycling in iron oxyhydroxide-rich microbial mats at Loihi Seamount. *Geomicrobiol J*. 26:639–647.
- Emerson D, Floyd MM. 2005. Enrichment and isolation of iron-oxidizing bacteria at neutral pH. *Environ Microbiol*. 397:112–123.
- Emerson D, Moyer CL. 1997. Isolation and characterization of novel iron-oxidizing bacteria that grow at circumneutral pH. *Appl Environ Microbiol*. 63:4784–4792.
- Emerson D, Revsbech NP. 1994. Investigation of an iron-oxidizing microbial mat community located near Aarhus, Denmark – field studies. *Appl Environ Microbiol*. 60:4022–4031.
- Ferris FG. 2005. Biogeochemical properties of bacteriogenic iron oxides. *Geomicrobiol J*. 22:79–85.
- Gerke TL, Maynard JB, Schock MR, Lytle DL. 2008. Physiological characterization of five iron tubercles from a single drinking water distribution system: possible new insights on their formation and growth. *Corros Sci*. 50:2030–2039.
- Gerke TL, Scheckel KG, Ray RI, Little BJ. 2012. Can dynamic bubble templating play a role in corrosion product morphology? *Corrosion*. 68:025004-1–025004-7.
- Guillard RR, Ryther JH. 1962. Studies of marine planktonic diatoms .1. *Cyclotella nana* Hustedt, and *Detonula confervacea* (Cleve) Gran. *Can J Microbiol*. 8:229–239.
- Guillard RRL. 1975. Culture of phytoplankton for feeding marine invertebrates. In: Smith WL, Chanley MH, editors. *Culture of marine invertebrate animals*. New York, NY: Plenum Press; p. 26–60.
- Handley KM, Boothman C, Mills RA, Pancost RD, Lloyd JR. 2010. Functional diversity of bacteria in a ferruginous hydrothermal sediment. *ISME J*. 4:1193–1205.
- Herrera LK, Videla HA. 2009. Role of iron-reducing bacteria in corrosion and protection of carbon steel. *Int Biodeter Biodegr*. 63:891–895.
- Hicks RE. 2007. Structure of bacterial communities associated with accelerated corrosive loss of port transportation infrastructure. Final report for Great Lakes Maritime Research Institute. Great Lakes Maritime Research Institute, MN: Great Lakes Maritime Research Institute. Available from: <http://www.glmri.org/research/completedstudies/Tab5.pdf>.
- James RE, Ferris FG. 2004. Evidence for microbial-mediated iron oxidation at a neutrophilic groundwater spring. *Chem Geol*. 212:301–311.
- Kobrin G. 1976. Corrosion by microbiological organisms in natural waters. *Mater Performance*. 15:38–43.
- Langley S, Gault AG, Ibrahim A, Takahashi Y, Renaud R, Fortin D, Clark ID, Ferris FG. 2009. Sorption of strontium onto bacteriogenic iron oxides. *Environ Sci Technol*. 43:1008–1014.

- Larsen I, Little BJ, Nealson K, Ray RI, Stone A, Tian J. 1998. Manganite reduction by *Shewanella putrefaciens* mr-4. *Am Mineral*. 83:1564–1572.
- Larsen O, Postma D. 2001. Kinetics of reductive bulk dissolution of lepidocrocite, ferrihydrite, and goethite. *Geochim Cosmochim Acta*. 65:1367–1379.
- Lee JS, Ray RI, Lemieux EJ, Falster AU, Little BJ. 2004. An evaluation of carbon steel corrosion under stagnant seawater conditions. *Biofouling*. 20:237–247.
- Little BJ, Gerchakov SM, Udey L. 1987. A method for the sterilization of natural seawater. *J Microbiol Methods*. 7:193–200.
- Little BJ, Lee JS. 2007. Microbiologically influenced corrosion. Hoboken, NJ: Wiley.
- Little BJ, Ray RI, Lee JS. 2010. Tubercles and localized corrosion on carbon steel. *Corros Manage Mag*. 98:12–15.
- Little BJ, Wagner PA, Hart KR, Ray RI, Lavoie DM, Nealson K, Aguilar C. 1997. The role of metal-reducing bacteria in microbiologically influenced corrosion. *CORROSION/97*, New Orleans, LA. Paper no. 215. Houston, TX: NACE International.
- Lovley DR, Stolz JF, Nord GL, Phillips EJP. 1987. Anaerobic production of magnetite by a dissimilatory iron-reducing microorganism. *Nature*. 330:252–254.
- McBeth JM, Little BJ, Ray RI, Farrar KM, Emerson D. 2011. Neutrophilic iron-oxidizing ‘Zetaproteobacteria’ and mild steel corrosion in nearshore marine environments. *Appl Environ Microbiol*. 77:1405–1412.
- McNeil MB, Odom AL. 1994. Thermodynamic prediction of microbiologically influenced corrosion (MIC) by sulfate-reducing bacteria (SRB). In: Kearns JR, Little BJ, editors. *Microbiologically influenced corrosion testing*. Philadelphia, PA: ASTM; p. 173–179.
- Miot J, Benzerara K, Obst M, Kappler A, Hegler F, Schadler S, Bouchez C, Guyot F, Morin G. 2009. Extracellular iron biomineralization by photoautotrophic iron-oxidizing bacteria. *Appl Environ Microbiol*. 75:5586–5591.
- Myers C, Nealson KH. 1988. Bacterial manganese reduction and growth with manganese oxide as the sole electron acceptor. *Science*. 240:1319–1321.
- Nealson K, Little BJ. 1997. Breathing manganese and iron: solid-state respiration. In: Neidleman SL, Laskin AI, editors. *Advances in applied microbiology*. San Diego, CA: Academic Press; p. 213–239.
- Ray R, Little B. 2003. Environmental electron microscopy applied to biofilms. In: Lens P, Moran AP, Mahony T, Stoodley P, O’Flaherty V, editors. *Biofilms in medicine, industry and environmental biotechnology*. London: IWA; p. 331–351.
- Ray RI, Lee JS, Little BJ. 2009. Factors contributing to corrosion of steel pilings in Duluth-Superior Harbor. *Corrosion*. 65:707–717.
- Ray RI, Lee JS, Little BJ, Gerke TL. 2011. The anatomy of tubercles on steel. *CORROSION/2011*, Houston, TX. Paper no. 11217. Houston, TX: NACE International.
- Roden EE, McBeth JM, Blothe M, Percak-Dennett EM, Fleming EJ, Holyoke RR, Luther GW, Emerson D, Schieber J. 2012. The microbial ferrous wheel in a neutral pH groundwater seep. *Front Microbiol*. 3:1–18.
- Sharpley JM. 1961. Microbiological corrosion in waterfloods. *Corrosion*. 17:92–96.
- Stookey LL. 1970. Ferrozine – a new spectrophotometric reagent for iron. *Anal Chem*. 42:779–781.
- Straub KL, Benz M, Schink B. 2001. Iron metabolism in anoxic environments at near neutral pH. *FEMS Microbiol Ecol*. 34:181–186.
- Szklarska-Smialowska Z. 2005. Pitting and crevice corrosion. Houston, TX: NACE International.
- Toner BM, Berquo TS, Michel FM, Sorensen JV, Templeton AS, Edwards KJ. 2012. Mineralogy of iron microbial mats from Loihi Seamount. *Front Microbiol*. 3:1–18.
- Wang JJ, Vollrath S, Behrends T, Bodelier PLE, Muyzer G, Meima-Franke M, Den Ouden F, Van Cappellen P, Laanbroek HJ. 2011. Distribution and diversity of *Gallionella*-like neutrophilic iron oxidizers in a tidal freshwater marsh. *Appl Environ Microbiol*. 77:2337–2344.
- Weiss JV, Emerson D, Megonigal JP. 2004. Geochemical control of microbial Fe(III) reduction potential in wetlands: comparison of the rhizosphere to non-rhizosphere soil. *FEMS Microbiol Ecol*. 48:89–100.